

Evolution Of The Thermal Cap In Two Wells From
The Salton Sea Geothermal System, California

Joseph N. Moore and Michael C. Adams

University of Utah Research Institute
Salt Lake City, Utah

ABSTRACT

The Salton Sea geothermal system is overlain by a thermal cap of low permeability rocks that restricts the upward movement of the high-temperature reservoir brines. Petrographic and fluid inclusion data from two wells show that the thermal cap in the southern part of the field consists of an upper layer of lacustrine and evaporite deposits with low initial permeabilities and a lower layer of deltaic sandstones. The sandstones were incorporated into the thermal cap as downward percolating fluids deposited anhydrite and calcite in the pore space of the rocks, reducing their permeabilities. During development of the thermal cap, base-metal sulfides, potassium feldspar and quartz veins were deposited by brines from higher temperature portions of the system.

INTRODUCTION

The Salton Sea geothermal system is located near the center of the sediment filled Salton Trough of southern California and Mexico. Mineral assemblages and textures formed in response to geothermal activity can be categorized as diagenetic or metamorphic (McKibben and Elders, 1985). Diagenetic processes occur at temperatures of less than about 250°C and have resulted in the recrystallization of the sheet silicates, and the deposition of anhydrite, carbonates, and sulfides in the pore space of the sediments. The reduction in the permeabilities of the shallow sediments caused by the deposition of these pore filling minerals has led to the development of a thick thermal cap, or zone of conductive heating, over the reservoir (Younker et al., 1982). Metamorphic processes occurring in the reservoir, where temperatures range from 250° to 365°C, have led to the development of hornfelsic textures and mineral assemblages typical of the greenschist facies (Muffler and White, 1969). Fluids encountered at the depths where these metamorphic processes are occurring have salinities of up to 25 weight percent (Hedgeson, 1968).

In contrast to the deep portions of the Salton Sea geothermal system, little data has been presented on the temperatures and salinities of the brines that have charac-

terized the upper parts of the geothermal field. Furthermore, because there is evidence that conditions within the geothermal system have changed with time (Skinner et al., 1967; Huang, 1977; Andes and McKibben, 1987), the present borehole temperatures and fluids may not accurately reflect the conditions associated with the alteration of the shallow sediments. Alternatively, this data can be obtained from fluid inclusions contained within the authigenic minerals. In this paper we describe the results of fluid inclusion and petrographic studies of two boreholes drilled in the southern part of the field (Fig. 1). The samples were provided by Unocal.

LITHOLOGIC AND MINERALOGIC RELATIONSHIPS

The rocks within the Salton Sea geothermal system can be divided into an upper sequence of lacustrine claystone and evaporite deposits and a lower sequence of deltaic sandstones, siltstones and shales (Randall, 1974). Figure 2 details the lithologies and mineral assemblages found in the upper parts of the wells studied by us. These lithologic columns are based on an examination of drill chip samples collected at 6 or 9 m (20 or 30 foot) intervals.

The primary and secondary minerals we observed (Fig. 2) are similar to those found in other parts of the field (e. g. Muffler and White, 1969; McDowell and Elders, 1979, 1980, 1983). With increasing depth, the secondary assemblages are characterized by: 1) anhydrite, calcite, interlayered illite/smectite, and interlayered chlorite/-smectite (interlayered illite/smectite zone: 0-222 m, Well A; 0-241 m, Well B); 2) chlorite, illite, interlayered chlorite-/smectite, calcite, anhydrite, potassium feldspar, quartz, sphene, and base-metal sulfides (chlorite-calcite zone: 222-616 m, Well A; 241-789 m, Well B); and 3) epidote, calcite, chlorite, quartz, potassium feldspar, albitic plagioclase, anhydrite, illite, and sphene (chlorite-epidote-calcite zone: 616-1646 m, well A; 789-1292 m, Well B). Traces of pyrite and hematite occur throughout these zones.

FLUID INCLUSION DATA

Fluid inclusions in anhydrite, sphalerite and vein quartz were studied. In the lacustrine deposits, anhydrite occurs as rosettes in the claystones and as aggregates associated with calcite in the evaporite beds. In the deltaic deposits, anhydrite and calcite cement the sandstones above 387 m in well A and 351 m in well B. At greater depths, anhydrite-rich zones are restricted to a few narrow intervals.

Sphalerite occurs in significant amounts (up to several percent) as a cement in the sandstones between 341 and 387 m in well A and from 277 to 360 m and 424 to 433 m in well B. In places, the sphalerite contains inclusions of anhydrite, suggesting that it has replaced preexisting anhydrite cement. Rocks between depths of 300 and 600 m also commonly contain secondary potassium feldspar after detrital plagioclase. The significance of these mineral assemblages is discussed below.

Quartz veins containing minor barite, chlorite, hematite, and traces of galena, sphalerite, calcite and anhydrite occur between depths of 305 and 378 m in well B (Fig. 2). Barite, in particular, is an uncommon mineral in the Salton Sea geothermal system. In these veins, it is found as embayed crystals surrounded by quartz.

The petrographic relationships suggest that the deposition of anhydrite began prior to both sphalerite cementation and quartz veining. Thus, fluid inclusions in anhydrite can potentially provide information on the temperatures and compositions of the brines since the early evolution of the thermal system. As discussed below, inclusions in sphalerite and vein quartz provide information associated with the episodic upwelling of brines from deeper parts of the system. Most of the fluid inclusion data from the Salton Sea geothermal system is of this latter type (Huang, 1977; Freckman, 1978; Andes and McKibben, 1987; Roedder and Howard, 1987).

All the fluid inclusions examined in this study were liquid-rich and contained a small vapor bubble that occupied about 20 percent of the inclusion volume at room temperature. Most had maximum dimensions in the range of 2 to 10 microns. No evidence of a separate gas phase was observed in these inclusions and, with the exception of anhydrite from 168-177 m in well B, none of the inclusions found contained any solid phases. In order to assure the validity of our data, fluid inclusions in anhydrite from three depth intervals were systematically overheated to determine their stretching characteristics. These experiments demonstrated that stretching caused by laboratory heating is not likely to have affected the results reported in this study.

In addition, the gas contents of inclusions in ten samples were analyzed by mass spectrometry using the techniques

described by Sommer et al. (1985). Methane, ethane, propane and carbon dioxide were detected in primary inclusions in sphalerite and quartz. Inclusions in anhydrite contained mainly carbon dioxide and methane.

Anhydrite suitable for fluid inclusion measurements typically occurs as cleavage fragments up to 2 mm across. Typically several generations of secondary or pseudo-secondary inclusions are present. Primary inclusions containing a small (<1 micron), unidentified birefringent daughter mineral were observed in samples from 168-177 m in well B. These inclusions form three dimensional arrays that define growth zones in the cleavage fragments.

The homogenization temperatures of fluid inclusions in anhydrite are plotted against depth in Figure 3A. The data show that irrespective of the origin of the inclusions in these samples, homogenization temperatures vary little within each depth interval, and that the two wells record similar thermal profiles. No pressure correction has been applied to these data because of the shallow depths.

Ice melting temperatures of fluid inclusions in anhydrite (Fig. 3B) range from -21.4° to -4.7° C. Liquid was observed in some of the larger inclusions at temperatures near -50° C (first melting), indicating that the inclusion fluids are enriched in CaCl_2 . For reference, melting point depressions ranging from 4.7° to 20.8° C correspond to salinities of 7.4 to 23.2 equivalent weight percent NaCl (Potter et al., 1978).

Fluid inclusions in sphalerite suitable for freezing and heating measurements were found in a few crystals from two depth intervals in well B. These inclusions are primary, forming small isolated groups or three-dimensional arrays that parallel color banding. The inclusions yielded homogenization temperatures ranging from 179° to 223° C (Fig. 3A), and ice melting temperatures (Fig. 3B) ranging from -12.0 to -10.0° C (16.0 to 14.0 equivalent weight percent NaCl).

Data were obtained on primary (refer to Figs. 3A and B) and secondary inclusions of vein quartz. The primary inclusions occur in three dimensional arrays that define growth zones. Homogenization temperatures of these inclusions range from 194° to 242° C (Fig. 3A). Because of their small size (1 to 3 microns) only a few freezing point depressions were measured. The ice melting temperatures ranged from -13.9° to -9.2° C (17.8 to 13.1 equivalent weight percent NaCl).

Secondary inclusions have homogenization temperatures ranging from 189° to 210° C and ice melting temperatures that vary from -16.5° to -0.7° C (20.0 to 1.2 equivalent weight percent NaCl). The high-salinity inclusions have freezing point depressions similar to the brines trapped in anhydrite at these depths and thus may represent locally

derived fluids. The low-salinity fluids may represent condensate mixed with a small amount of the higher salinity brines.

DISCUSSION

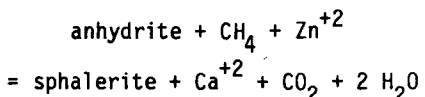
The data described above suggest that the evolution of the rocks in the shallow portions of the two wells studied involved four distinct processes. These include: 1) the formation of secondary minerals through low- to moderate-temperature isochemical reactions; 2) the progressive downward cementation of the sandstones by anhydrite and calcite; 3) the influx of metal-bearing brines; and 4) the development of fracture permeability. The initial heating of the sediments is reflected in the formation of anhydrite after gypsum and the recrystallization of the sheet silicates as discussed by Muffler and White (1969). In contrast, the anhydrite + calcite cement in the deltaic sandstones could not have formed from the fluids or detrital components originally present in these rocks. However, the fluids in the overlying lacustrine rocks would have been enriched in both sulfate and bicarbonate. Because calcite and anhydrite display retrograde solubilities, heating of downward moving sulfate and carbonate ions would have resulted in the deposition of these minerals in the sandstones immediately underlying the lacustrine deposits. With time, continued diffusion of sulfate and carbonate would have led to a progressive thickening of the anhydrite + calcite cemented sandstones.

The fluid inclusions in anhydrite record temperature profiles characterized by high gradients through the upper 323 m in well A and 341 m in well B. Using the average homogenization temperature of 247°C for samples from a depth of 332-341 m in well B, and a mean annual air temperature of 22.5°C (Imperial Irrigation District, 1982), the calculated average gradient to this depth is 0.66°C/m. Younker et al. (1982) have shown that such high gradients are indicative of heat transfer by conduction through rocks of low permeability. This calculated gradient and the mineralogic relationships suggest that the thermal cap extends to the base of the anhydrite + calcite cemented sandstones. In contrast, homogenization temperatures of inclusions in well A between 460 and 622 m are nearly constant with depth, implying that heat is transferred through these rocks by convection (Younker et al., 1982).

The secondary potassium feldspar and sphalerite cement found in the lower part of the thermal cap could not have been formed by the fluids that deposited the anhydrite in the sandstones. The replacement of plagioclase by potassium feldspar involved the addition of K and removal of Na from the rocks. Because the K/Na ratio of geothermal waters increases with increasing temperature (Fournier and Truesdell, 1973), the formation of potassium feldspar in the shallow

deltaic rocks must have resulted from the influx of brines derived from higher-temperature portions of the geothermal system. These fluids would also have been a likely source of zinc, lead, and copper.

As discussed above, our observations suggest that the sphalerite cement found in the deltaic sandstones has replaced pre-existing anhydrite cement. Reduction of the sulfate to sulfide could have occurred by several different mechanisms. However, reduction by pre-existing sulfides or anaerobic bacteria is not likely in this case. Alternatively, the sulfate could have been reduced by hydrocarbons carried in solution by the upwelling brines according to the reaction (Anderson, 1983):



We infer from the widespread occurrence of sphalerite cement that matrix permeabilities were relatively high during its deposition. In contrast, the formation of veins implies lower matrix permeabilities and fracture-dominated fluid flow (Elders, 1979). The occurrence of barite in these veins suggests that some mixing of the pore and vein fluids occurred. As noted by Barnes (1983) in his discussion of Mississippi Valley lead-zinc deposits, the deposition of barite would most likely occur where barium-bearing solutions encountered a sulfate-rich groundwater or where oxidation of sulfide to sulfate in solution can occur. As discussed above, sulphate-bearing pore fluids must have been present in the sandstones in the upper part of the deltaic section and could have mixed with the rising vein fluids. Later, these fluids would have been purged from the veins as upward flow continued, causing dissolution of early barite and deposition of sulfides, hematite and additional quartz from further cooling.

SUMMARY AND CONCLUSIONS

Fluid inclusion data and petrographic studies have been used to reconstruct the evolution of the rocks in the shallow portions of two wells drilled in the southern part of the Salton Sea geothermal system. The initial heating of these rocks resulted in the formation of anhydrite after gypsum and the formation of secondary phyllosilicates. Anhydrite and calcite were also deposited directly from the pore fluids as a cement in the underlying deltaic sandstones. Cementation of the sandstones progressed downward, reducing their permeabilities and leading to a thickening of the thermal cap with time. Fluid inclusion homogenization temperatures in anhydrite increase systematically with depth through the thermal cap. Variations in the salinities of these fluid inclusions demonstrate

that some mixing of downward-percolating brines and reservoir fluid took place. However, the velocities of the descending waters were apparently not high enough to disturb the thermal gradient.

The influx of brines from higher temperature portions of the geothermal system occurred episodically during development of the thermal cap. Movement of these brines through the thermal cap resulted in the deposition of potassium feldspar and sphalerite cement and in the formation of quartz veins.

ACKNOWLEDGEMENTS

Funding for this project was provided by the Department of Energy under Contract Number DE-AC03-84SF12196. We would like to thank R. Dondanville and G. Suemnicht of Unocal for providing the samples. M. Sommer performed the gas analyses.

REFERENCES

Anderson, G. M. (1983) Some geochemical aspects of sulfide precipitation in carbonate rocks. In: International Conference on Mississippi Valley Type Lead-Zinc Deposits. Proc. Vol. (Edited by Kisvarsanyi, G., Grant, S. K., Pratt, W. P. and Koenig, J. W.), pp. 61 -76. University of Missouri-Rolla, Rolla, MO.

Andes, J. P., Jr., and McKibben, M. A. (1987) Thermal and chemical history of mineralized fractures in cores from the Salton Sea scientific drilling project (abstract). Eos Trans. AGU. 68, 439.

Barnes, H. L. (1983) Ore-depositing reactions in Mississippi Valley-type deposits. In: International Conference on Mississippi Valley Type Lead-Zinc Deposits. Proc. Vol. (Edited by Kisvarsanyi, G., Grant, S. K., Pratt, W. P. and Koenig, J. W.), pp. 77 - 85. University of Missouri-Rolla, Rolla, MO.

Elders, W. A. (1979) The geological background of the geothermal fields of the Salton Trough. In: Geology and Geothermics of the Salton Trough (Edited by Elders, W. A.), Campus Museum Contribution, University of California, Riverside, Ca. 5, pp. 1 - 19.

Fournier, R. O., and Truesdell, A. H. (1973) An empirical Na-K-Ca geothermometer for natural waters. Geochim. Cosmochim. Acta. 37, 1255 - 1275.

Freckman, J. T. (1978) Fluid inclusion and oxygen isotope geothermometry of rock samples from Sinclair No. 4 and Elmore No. 1 boreholes, Salton Sea geothermal field, Imperial Valley, California, U.S.A. M.S. Thesis, University of California, Riverside, CA. 66 pp.

Haas, J. L., Jr. (1971) The effect of salinity on the maximum thermal gradient of a hydrothermal system at hydrostatic pressure. Econ. Geol. 66, 940 - 946.

Huang, C. I. (1977) Fluid inclusion study of well cuttings from Magmamax No. 2 drillhole, Salton Sea geothermal area, California (abstract). Econ. Geol. 72, 730.

Helgeson, H. C. (1968) Geologic and thermodynamic characteristics of the Salton Sea geothermal system. Am. J. Sci. 266, 3, 129-166.

Imperial Irrigation District, Imperial Valley Annual Weather Summary (1982) Monthly high, low, and mean temperatures and rainfall, 1914-1982. Community and Special Services, Imperial Irrigation District, El Centro, CA. 19 pp.

McDowell, S. D., and Elders, W. A. (1979) Geothermal metamorphism of sandstone in the Salton Sea geothermal system. In: Geology and Geothermics of the Salton Trough (Edited by Elders, W. A.), Campus Museum Contribution, University of California, Riverside, CA. 5, pp. 70 - 76.

McDowell, S. D., and Elders, W. A. (1980) Authigenic layer silicate minerals in borehole Elmore 1, Salton Sea geothermal field, California, U.S.A. Cont. Mineral. Pet. 74, 293 - 310.

McDowell, S. D., and Elders, W. A. (1983) Allogenic layer silicate minerals in borehole Elmore No. 1, Salton Sea geothermal systems. Am. Mineral. 68, 1146 - 1159.

McKibben, M. A., and Elders, W. A. (1985) Fe-Zn-Cu-Pb mineralization in the Salton Sea geothermal system, Imperial Valley, California. Econ. Geol. 80, 539 - 559.

Muffler, L. J. P., and White, D. E. (1969) Active metamorphism of upper Cenozoic sediments in the Salton sea geothermal field and the Salton Trough, southeastern California. Geol. Soc. Am. Bull. 80, 157 - 182.

Potter, R. W., II, Clyne, M. A., and Brown, D. L. (1978) Freezing point depression of aqueous sodium chloride solutions. Econ. Geol. 73, 284 - 285.

Randall, W. (1974) An analysis of the subsurface structure and stratigraphy of the Salton Sea geothermal anomaly, Imperial Valley, California. Ph.D. thesis University of California, Riverside, CA. 92 pp.

Skinner, B. J., White, D. E., Rose, H. J., and Mays, R. E. (1967) Sulfides associated with the Salton Sea geothermal brine. Econ. Geol. 62, 316 - 330.

Sommer, M. A., II, Yanover, R. N., Bourcier, W. L., and Gibson, E. K. (1985) Determination of H_2O and CO_2 concentrations in fluid inclusions in minerals using laser decrepitation and capacitance manometer analysis. Anal. Chem. 57, 449 - 453.

Younker, L. W., Kasameyer, P. W., and Tewhey, J. D. (1982) Geological, geophysical, and thermal characteristics of the Salton Sea geothermal field, California. J. of Volcan. and Geothermal Res. 12, 221 - 258.

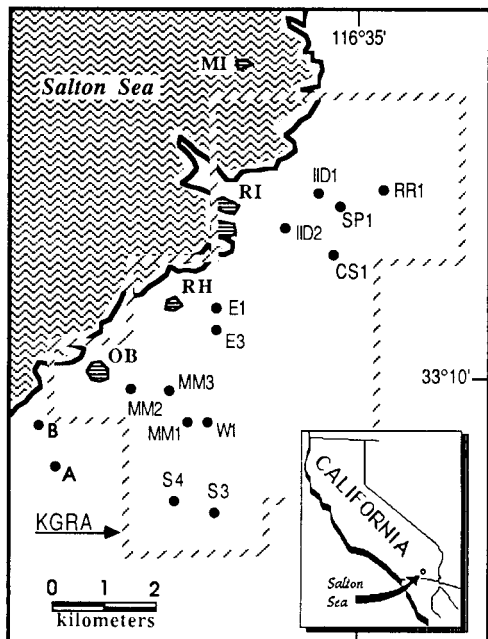


Fig. 1.

Well locations in the Salton Sea geothermal field. Wells: CS = California State; E = Elmore; MM = Magmamax; S = Sinclair; SP = Sportsman; W = Woolsey. A and B are the locations of the wells described in this study. Rhyolite domes: MI = Mullet Island; OB = Obsidian Butte; RH = Rock Hill; RI = Rock Island. The hachured line shows the boundary of the original Salton Sea Known Geothermal Resource Area (KGRA). Modified from McDowell and Elders (1980).

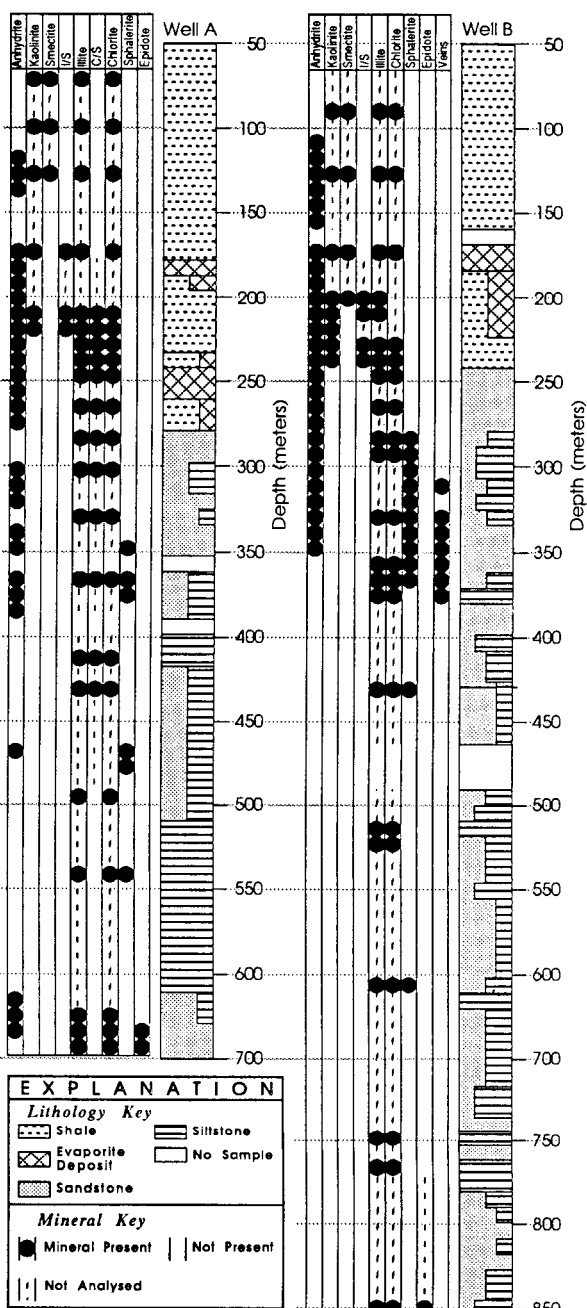


Fig. 2.

Lithologies and mineral distributions in the interlayered illite/smectite and chlorite - calcite zones of the two wells studied. I/S and C/S refer to interlayered illite/smectite and chlorite/smectite respectively.

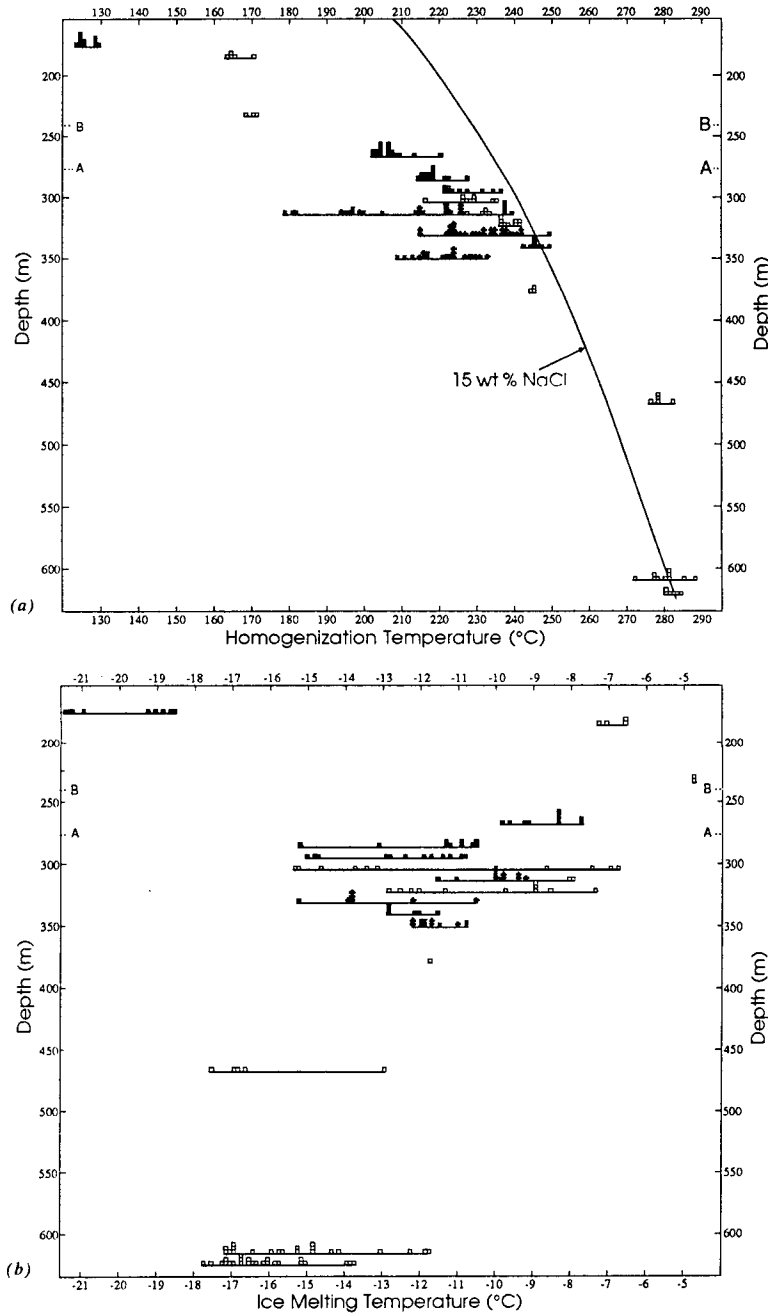


Fig. 3A.

Homogenization temperature vs. depth of fluid inclusions in anhydrite, sphalerite, and quartz. Symbols: anhydrite = open squares, Well A; filled squares, Well B; + = quartz, Well B; X = sphalerite, Well B. The baselines of the histograms are located at the lowermost limit of the sample interval. Tick marks labeled A and B indicate the depth to the base of the lacustrine deposits in the two wells. The boiling point curve for a 15 weight percent NaCl solution (Haas, 1971) is also shown for reference. B. Freezing point depression vs. depth for fluid inclusions in anhydrite. Refer to Fig. 3A for an explanation of the symbols.